Original Article

Ahmed Wagih*, Merima Hasani, Stephen A. Hall, Vladimir Novak and Hans Theliander

In situ microstructural evolution of spruce wood during soda pulping using synchrotron X-ray tomography

https://doi.org/10.1515/hf-2021-0204
Received October 4, 2021; accepted February 16, 2022;
published online March 16, 2022

Abstract: A new laboratory reactor to perform *in situ* studies of structural changes in wood during soda pulping using synchrotron X-ray tomography is presented. The reactor is of recirculation type to provide stable reaction conditions and mimic the industrial situation. Experiments have been performed using this reactor *in situ* at a synchrotron microtomography beamline to provide sequences of 3D images from which measurement of wood cell wall thickness have been possible for the first time. The results showed that the cell wall thickness increased significantly in the early stage of pulping (<10 min), which is due to the transportation of cooking chemicals through the tracheids, resin channels and pits into the cell wall, which is swollen with the increased pH. Subsequently, the cell wall thickness reduces over the processing time up to 60 min with a high rate, which is inferred to be due to the dissolution and transport of lignin and hemicellulose from the secondary walls, allowing for better transportation of active chemicals deep through the cell wall layers. After 60 min processing, the cell wall thickness reduction rate reduced, as dissolution of lignin and hemicelluloses from the cell walls ceased, while the remaining dissolution occurs mainly at the middle lamella.

Keywords: compression wood; microstructure; soda pulping; synchrotron X-ray tomography.

***Corresponding author: Ahmed Wagih,** Forest Products and Chemical Engineering, Chalmers University of Technology, SE-412 96 Gothenburg, Sweden; Mechanical Design and Production Department, Faculty of Engineering, Zagazig University, P.O. Box 44519, Zagazig, Egypt; and King Abdullah University of Science and Technology, Thuwal, Saudi Arabia, E-mail: ahmedwagih@zu.edu.eg. https://orcid.org/0000-0003-2782-6198
Merima Hasani and Hans Theliander, Forest Products and Chemical Engineering, Chalmers University of Technology, SE-412 96 Gothenburg, Sweden; and Wallenberg Wood Science Center, Chalmers University of Technology, SE-41296 Gothenburg, Sweden
Stephen A. Hall, Division of Solid Mechanics, Lund University, Lund, Sweden; and Lund Institute of Advanced Neutron and X-ray Science, Lund, Sweden
Vladimir Novak, Paul Scherrer Institute, Swiss Light Source, Forschungsstr. 111, 5232 Villigen PSI, Switzerland

1 Introduction

Chemical pulping, including kraft and soda pulping, is the most common technology for paper pulp production and has been the "work horse" of this industry for the last 60 years. During the pulping process, complex chemical reactions occur leading to partial depolymerization and solubilization of lignin and hemicelluloses. Different underlying phenomena, involving chemical reaction kinetics, solubility and mass transport of wood tissue components, govern the course of the pulping process. The reaction mechanisms (and their intermediates and products) are well addressed in the literature (e.g. Chakar and Ragauskas 2004; Gierer 1980; Gellerstedt, Majtnerova, and Zhang 2004; Santos et al. 2013; Sjöström 1977). Moreover, the characterization of the dissolved lignin is well addressed and reported (e.g. Baptista, Robert, and Duarte 2006; Labidi, Robert, and Pla 1993; Robert et al. 1984). Additionally, the evolution of fiber quality and their mechanical properties after kraft pulping has been extensively investigated (e.g. Tikka and Kovasin 1990). However, the solubilization kinetics and mass transfer details of the delignification mechanisms, their sequences and sub-processes, such as mass transport of cooking chemicals in the cell wall and to the middle lamella along with the mass transport of dissolved wood constituents, are less well addressed. Consequently, there is no kinetic delignification model based on first principles available, as deep understanding of the abovementioned mass transport is of crucial importance for the development of such a model. An important step towards obtaining the required deeper understanding is to study the morphological changes of cell walls and middle lamella during a pulping process. Wagih et al. (2021)

investigated these aspects using *ex situ* X-ray tomography of wood samples extracted at different stages of the pulping process. However, the approach was limited by the *ex situ* analysis of the different samples from each specific stage of the process. This work aims for a deeper understanding through *in situ* experiments where the processes can be followed in the same sample through the pulping process.

X-ray Tomography (XRT) is an efficient 3D visualization tool that has been found to be useful in many areas of research, such as medicine, biology, material science and nanoscience (e.g., Ebner et al. 2013; Harry et al. 2014; Maire and Withers 2014; Wagih et al. 2019). Using this technique, a 3D representation of a sample can be reconstructed from large number of 2D projections at different rotation angles, which allows a nondestructive quantitative analysis of the microstructure inside a sample and monitoring of structural changes during sample evolution (e.g., during chemical reaction and/or mass transport of constituents) (Villevieille et al. 2015). Today, with the vast progress in the implementation of XRT, a wide spectrum of length scales from tens of nanometers to millimeter size are applied using lab or synchrotron based measurements (e.g., Scheel et al. 2008; Withers 2007). For example, entire plant cycles occurring over weeks or months have been studied using lab XRT machines (Ahmed et al. 2016), whereas fast events, such as the flying mechanism of insects, that occur in milliseconds have been studied using synchrotron XRT (Walker et al. 2014). *In situ* investigations of, for example, tests on materials at high temperatures, under mechanical loads and during solidification of metals are currently achievable using synchrotron XRT (e.g., Bale et al. 2013; Villevieille et al. 2015).

Regarding studies on wood structures, the wood anatomy at the submicron level has been investigated using XRT (e.g., Van den Bulcke et al. 2008). The density evolution of wood when subjected to moisture and heat has also been studied (Derome et al. (2011) and Lazarescu, Watanabe, and Avramidis (2010)) and Muzamal et al. (2016) studied the structural changes in wood after steam explosion. Recently, the micro- and nano-structure evolutions of spruce wood during soda pulping were studied (Wagih et al. 2021). In this previous study, the pulping process was interrupted every 30 min and a treated wood chip was extracted and washed to enable study of structural changes using lab XRT. A data analysis procedure was optimized to quantify the changes in the cell walls and the resin channels. The obtained results provided new information regarding the relation between the compositional (quantities of dissolved lignin and carbohydrates) and morphological changes in the wood tissue and cell walls, in particular. Despite the successful monitoring of the microstructural changes over the process time two main challenges were faced: (a) due to the saturation of the walls with water, the contrast between celluloses and lignin was reduced and hindered more comprehensive assessment of the observed changes (e.g. changes in the cell wall thickness and porosity); (b) the interruption of the experiment every 30 min exposed the samples to external conditions, which is known to affect the microstructure. Additionally, the fact that the XRT analysis was made every 30 min implies that only "snap-shots" of the structural changes were obtained and important information, in particular in the beginning of the operation associated with the fast delignification, might have been missed. Furthermore, different samples were analysed for each stage and so the true evolution of the microstructural changes could not be tracked. Therefore, to accurately investigate the structure evolution, imaging of samples while the experiment is running, is necessary, which presently is not possible with lab XRT due to the required fast acquisition times.

In this study, the evolution of microstructural changes in spruce wood during model alkaline (soda) pulping was visualized by monitoring the process *in situ* using synchrotron XRT. For this purpose, a reaction cell that enables *in situ* pulping in the XRT set-up was designed and manufactured. From the obtained *in situ* XRT images, the morphology during soda pulping process could be studied; among other things, the evolution of cell wall thickness could be estimated. Moreover, the different sub phases during soda pulping and their sequence was analyzed.

2 Materials and methods

2.1 Material

Norway spruce (*Picea abies*) wood chips (420 kg/m^3 density) of square cross section 5 × 5 mm^2 and 25 mm length were used. To ensure as similar as possible structure and geometry of the different samples used in this test campaign, a long wood chip of 150 mm length and 10 × 10 mm^2 cross section from the external part of a wood log (i.e. sapwood), where the major dimension is aligned with the longitudinal fiber direction, was cut. The samples for the study were extracted from the same wood log as in the previous study by Wagih et al. (2021), which had been stored in a freezer to preserve its state.

2.2 Reaction cell design

A small reaction cell for *in situ* study of structural changes in wood structure during soda pulping using synchrotron XRT was designed, as shown in Figure 1. The developed reaction cell, at

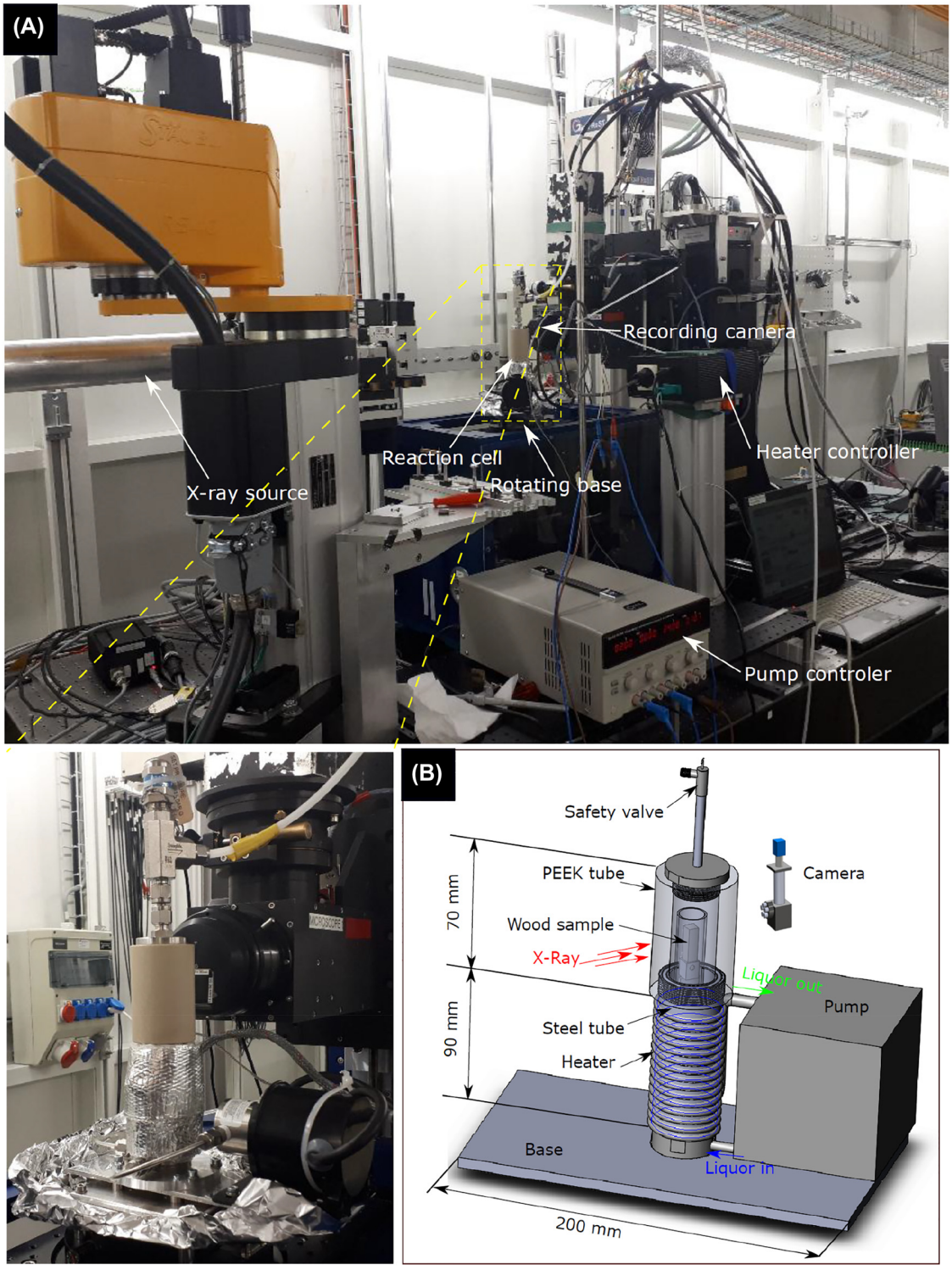

Figure 1: Experimental test set up showing the reaction cell mounted at the TOMCAT beamline.

least partly, mimics an industrial process for soda pulping: the wood chips were cooked inside the autoclave together with sodium hydroxide solution at high temperature and under pressure. Figure 2 shows schematic representation of the reaction cell mounted at the TOMCAT beamline at Swiss Light Source (Paul Scherrer Institut, Switzerland). The reactor was designed to have low X-ray attenuation materials to allow the penetration of the X-rays with minimum intensity loss, whilst still satisfying the constraints relating to the pressure and temperature conditions of the pulping process.

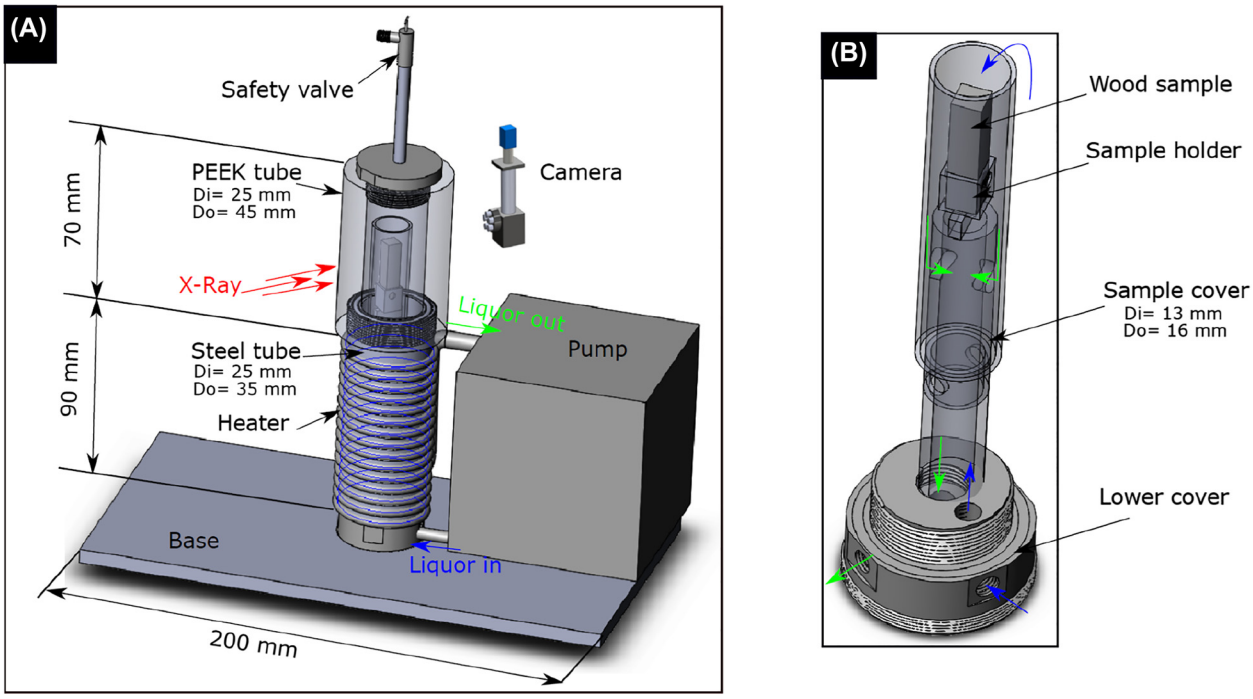

Figure 2: Schematic representation of the reaction cell clarifying the main components and dimensions in (A) and the liquor circulation system in (B). The blue arrows represent the liquor path to the sample while the green ones represent its path out to the pump. Di and Do in the figures refer to the inner and outer diameter of the tubes.

The reaction cell was constructed from a polyether ether ketone (PEEK) tube in the upper part of the cell where the reaction occurs and the X-rays pass through both the cell and the wood sample. PEEK was used due to its chemical and thermal stability, high service temperature, up to 260 °C, and high strength. Moreover, this material has good transmission of X-rays (~80%). The internal and external diameter of the PEEK tube were 25 and 45 mm, respectively. To avoid large deformations in the reaction cell, the reaction chamber was designed to have a PEEK tube in the upper part and a steel tube in the lower part; the latter had 25 mm internal diameter and 30 mm external diameter. The thickness of the tube wall was determined following pressure vessel design concepts. A magnetic heater coil was wrapped around the steel tube to heat up the system to the target temperature (130 °C) with heating rate at 50 °C/min using a heater controller device. The high heating rate was used to ensure that the target cooking temperature was reached within 3 min, i.e., except for a very short heating up period, the conditions were more or less isothermal. The sample was placed in a sample holder with the dimensions 5 × 5 mm^2 (see Figure 2B) and fixed using a screw over a hollow tube made of stainless steel with 8 and 12 mm internal and external diameters, respectively. The upper and lower ends of the reaction chamber were closed using steel covers with seals between the cover and the chamber to avoid pressure release and liquor leakage. The sample holder was mechanically fastened to the lower cover.

A key parameter in this experiment is the circulation of liquor around the sample to transport the dissolved component away from the surface. For this, an external pump was used to circulate the liquor around the system from the pump, through the sample holder (see green arrows in Figure 2) and then out from the reaction chamber in the area between the sample holder and the outer steel tube back to the pump, as shown in Figure 2B with blue arrows. A magnetic drive gear pump was used with PEEK driving and drive gears and stainless steel AISI 316 shafts and body (GA-X21J8FSA–IEC56B14–SEMH56-4C) provided by Techma GPM©. The pump can work with liquids up to a maximum temperature of 177 °C and pressure up to 21 bar, but higher pressures reduce the maximum operating temperature, which was, consequently, limited to 130 °C in the current experiment. A safety valve at the top of the reaction chamber was used to enable pressure release if it reaches more than 5 bars.

2.3 Soda pulping

Soda-pulping experiments on the wood chips in sodium hydroxide solution was performed with a concentration of 3% and a high solid to liquor ratio of 1:100 to have approximately constant concentration of hydroxide ions. The wood chips were charged to the reactor in dry phase. The temperature of the solution was kept constant and relatively low at 130 °C, which allowed for an easier monitoring of the progress of the process.

2.4 Synchrotron phase-contrast X-ray computed tomography

The *in situ* inspection of the wood microstructure was made using synchrotron XRT at the TOMCAT beamline (Swiss Light Source, Paul Scherrer Institut, Switzerland). The reaction cell was placed on the rotation stage of the beamline, as shown in Figure 1. The reaction cell with the sample inside was rotated from −90° to 90° in the X-ray beam

(50% white beam) with increments of 0.1° to acquire 1800 radiographic projections with 1.1 µm pixel size. Three different exposure times, 30, 100 and 300 ms, were considered for the radiographies during the first test to optimize this parameter with respect to the image quality and the process rate. The wet state of the samples and system requires longer exposure times to achieve good contrast in the saturated cell walls of the tracheids. However, the chemical reaction between wood and sodium hydroxide is fast, which requires short acquisition time to capture the fast changes in the structure during the reactions. The optimum exposure time for each radiographic projection was found to be 100 ms. Additionally, to overcome the noise caused by the continuous movement of air bubbles during the experiments resulting from the circulation of sodium hydroxide in the reaction cell, the pump was stopped during the collection of the X-ray projections and restarted again after the acquisition was completed. Based on previous *ex situ* inspections (Wagih et al. 2021), which demonstrated that fast structural change occur at the early stage of the test, the tomography measurements were performed every 10 min during the first hour of the test and then every 15 min in the second hour. Three tests were conducted with the same experimental conditions to ensure the repeatability of the test and the capability of recording images with the same quality. The in-house software at TOMCAT was used to reconstruct the obtained projections using the propagation-based phase contrast method (Paganin et al. 2002) and the gridrec algorithm (Marone and Stampanoni 2012). Tomography data were acquired to cover the upper part and the center of the sample with a 2 mm high field of view for each. Image-J was used to analyse the obtained reconstructions by measuring the cell wall thickness and to visualise the 3D volumes. At least 50 measurement of the double cell walls thickness for each sample were performed. Figure 3 shows an example of the image analysis that enabled the measurement of the cell walls in the wood sample just before the experiment was initiated (the samples were already submerged in the chemicals). An example cross-section through the reconstructed XRT image volume of the sample is shown in Figure 3A. These data were imported into the Image-J software and the histogram of the image was generated as shown in Figure 3B. The data were binarized to separate the air/liquid inside the sample from the cell walls, based on a threshold value defined from the histogram of the greyscale values in the whole image volume (the dark phase in Figure 3A is the air/liquid inside the sample, while the bright phase is the cell walls). Finally, the segmented image was obtained and the measurement of the cell wall thickness was performed between points at the borders of adjacent cell walls, as indicated in Figure 3D.

3 Results

Figure 4 shows transverse and longitudinal cross-section images through the XRT data volumes of the untreated wood sample before soda pulping. The typical wood

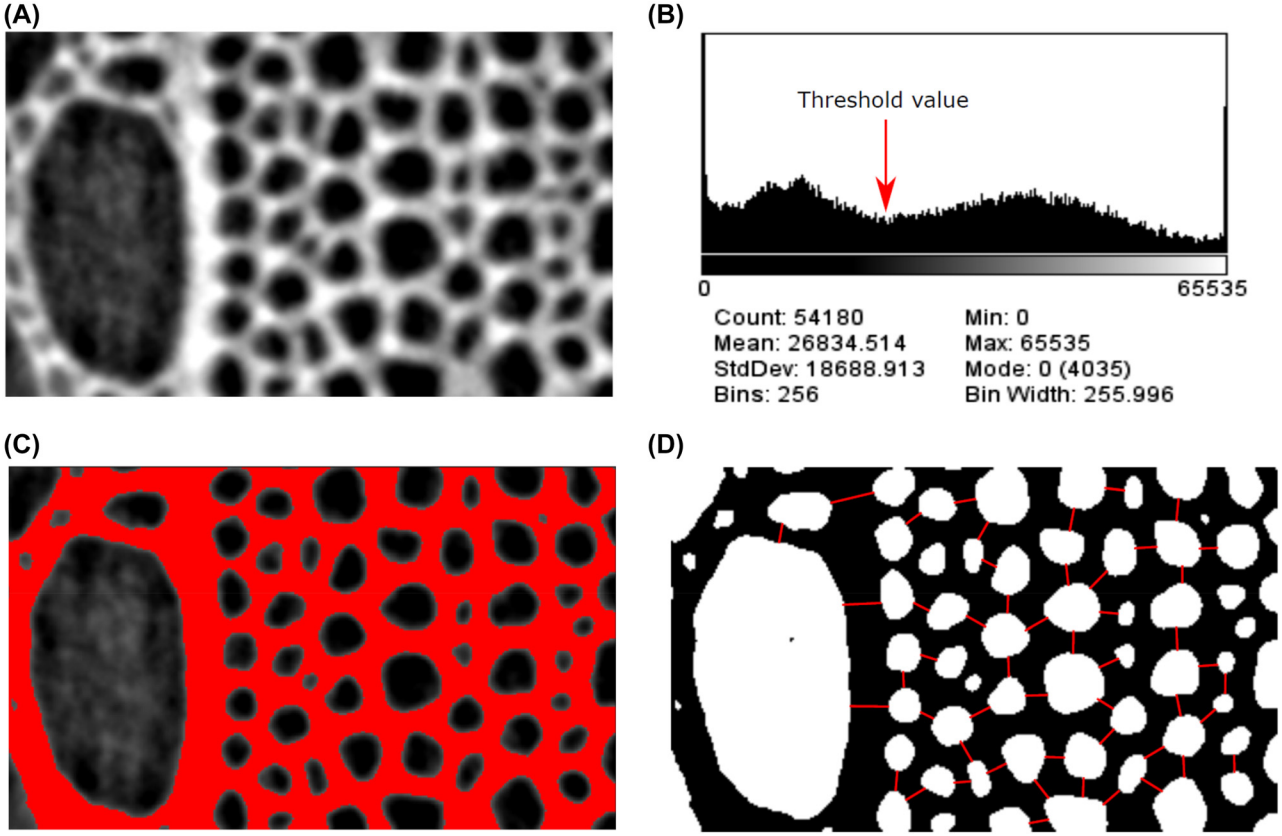

Figure 3: Image processing using image-J for double cell wall measurement.
(A) Example cross-section through the reconstructed XRT image volume, (B) histogram, (C) binarised image based on histogram segmentation and (D) binarised data with red lines indicating cell wall measurement lines. The red lines in (D) represents the distance between the two points used to measure the cell wall thickness.

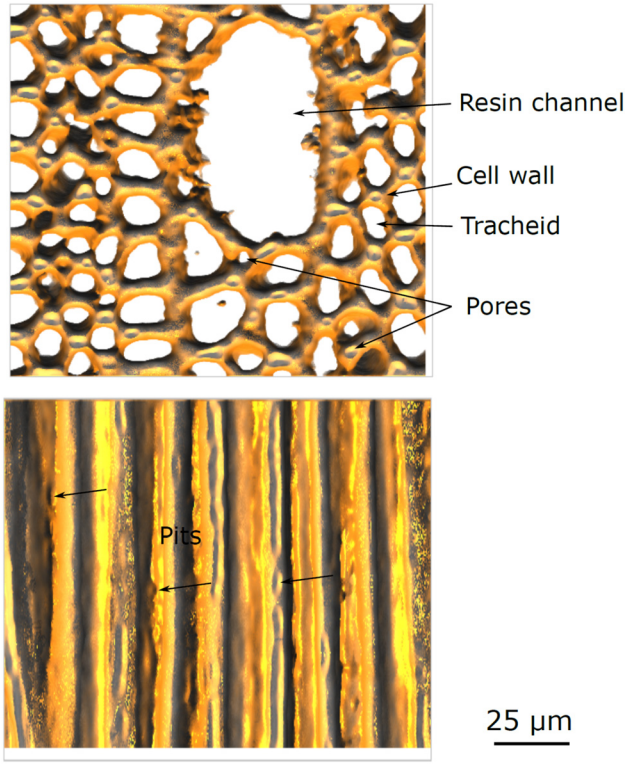

Figure 4: Transverse cross section and longitudinal XRT slices of untreated wood sample before soda pulping.

microstructure is observed with tracheids, cell walls and resin channels in the transverse cross sectional view, while bordered pits are observed in the longitudinal view. These pits form openings between tracheids through the cell walls with approximately 3 µm diameter and a membrane thickness of 1 µm (see, for example, Muzamal et al. 2016). Due to the small membrane thickness (less than two voxels), the complete structure of the openings was not visible (Muzamal et al. 2016; Walther and Thoemen 2009). The observed tracheids were of varying size and shape with elliptical and nonuniform transversal cross sections, which highlights that the wood considered was, just as in the earlier *ex situ* study, a so-called compression wood (Wagih et al. 2021). Additionally, as expected for a reaction wood, small pores could be observed in the cell corners.

It is noted that the samples for this study were not deliberately chosen to be compression wood. As often when working with a natural material as wood, natural variations are inevitable and sometimes hard to detect early on in a study, as was case with the earlier, related *ex situ* study (Wagih et al. 2021). In this previous work, both imaging and compositional studies indicated deviations from the standard wood resembling a compression wood. For the sake of comparison, the same wood material was chosen for this investigation. While delignification behavior of compression wood presumably reflects the higher content of condensed lignin, as well as a different content of non-cellulose polysaccharides relative to normal wood, monitoring it, nevertheless, provides valuable knowledge on delignification process in general, especially given the fact that compression wood is often a rather large tissue of the total wood area and knowledge of it, as such, gains a relevance for pulping.

Figure 5 shows 3D XRT images of spruce wood acquired *in situ* at different pulping times. At the beginning of the liquor addition (i.e. 0 min), there was no observable change in the microstructure; the same tracheid and cell wall shapes can be seen as in Figure 4. After 10 min pulping, the cooking chemicals were expected to have passed through tracheids, resin channels and pits to saturate the cell walls. Consequently, the cell walls should have absorbed a large amount of liquor, plus they are expected to swell in the alkaline environment, the resulting increase in cell wall thickness, associated reduction of tracheids inner diameter (i.e. the diameter of the lumen) and overall increase the volume of sample can be observed in the XRT images. Moreover, large deformation of tracheids and resin channels was observed. With further pulping up to 30 min, the cell wall thickness can be seen to have reduced and tracheid inner diameter started to increase. Also an initiation of separation between the cell walls at the middle lamella was observed. After 50 min, the tracheids inner diameter can be seen to have further increased and, consequently, the thickness of the cell walls further decreased. After 80 min, extensive separation between the cells can be seen, especially around the resin channel. Finally, after 120 min, the cell wall thickness was seen to be highly reduced with clear decohesion between cell walls around the resin channel.

4 Discussion

A new device that enables *in situ* (i.e., during the reaction process) monitoring with high resolution 3D XRT of the evolution of microstructure of wood during continuous soda pulping has been presented. With this device it has been possible to follow the pulping process for a small spruce wood sample and the dissolution of different wood components plus the resulting separation of the cells have been observed, as shown in Figure 5F. These observations agree well with previous *ex situ* experimental observations that employed a standard laboratory pulping set-up (Wagih et al. 2021) and, thus, confirms the efficiency of the new, *in situ* device to simulate the cooking operation.

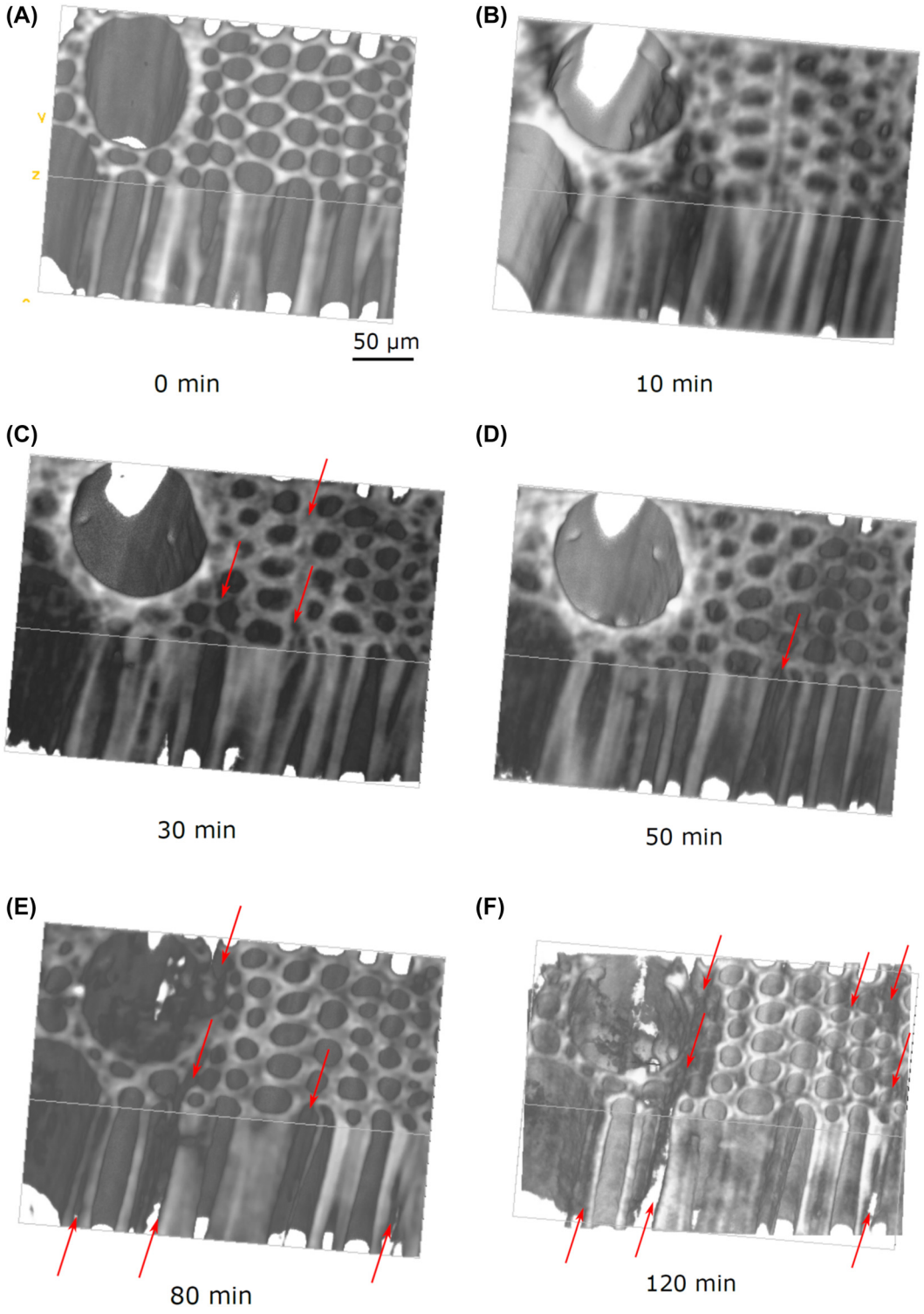

Figure 5: 3D rendered images of the *in situ* time-lapse 3D XRT of a spruce wood sample at different pulping times.
In (A), the microstructure corresponds to the sample just after adding the liquor inside the device. In (B)–(F), the microstructures of the wood sample at different pulping time is presented. The red arrows refer to the separation between cell walls.

Together with the previous study, the results indicate that, independent of experimental equipment used, fiber separation occurs after about 120 min pulping time.

In comparison to *ex situ* experiments, *in situ* studies provide additional information on changes in cell wall thickness. Figure 6 shows the estimated double cell wall

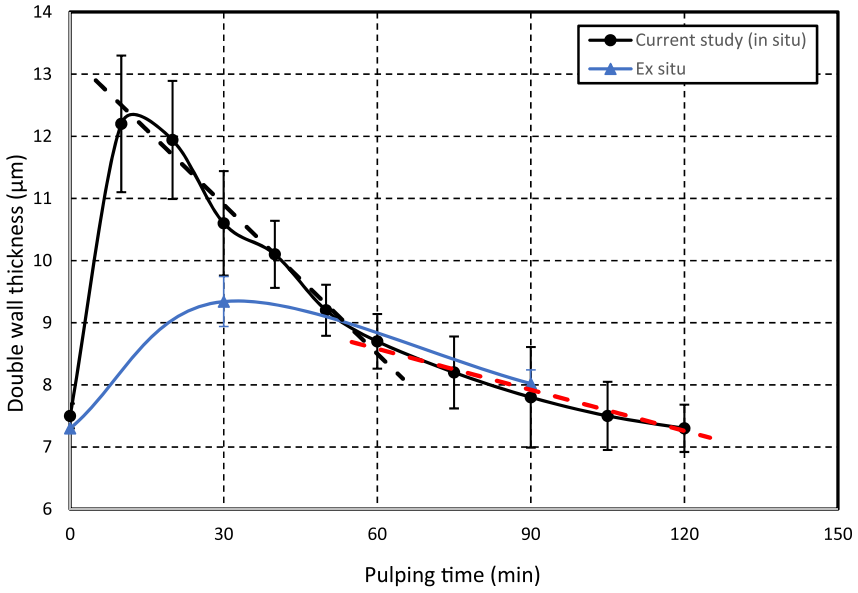

Figure 6: Evolution of cell wall thickness with pulping time. The *ex-situ* results are extracted from the authors' previous work (Wagih et al. 2021). The black and red dashed lines represent the linear fitting of the data between 20–60 min and between 60–120 min (the linear fitting is for clarifying the cell wall reduction rate).

thickness (cell wall–mid lamella–cell wall) of the investigated spruce wood sample at different times during the *in situ* soda cooking experiment, including a comparison with the data obtained in the earlier *ex situ* experiments, where the same wood log was used (Wagih et al. 2021). The cell wall thickness evolution agrees well in the later part of the process (after about 60 min), but at shorter times (60 min or shorter) there seems to be marked differences. For instance, at 30 min, the *ex situ* measured wall thickness was 9.34 µm, while the *in situ* measured thickness from the current study was 10.60 µm. The *ex situ* study could not capture the initial evolution (<30 min), but the *in situ* data show a significant increase in the double wall thickness from 7.5 to 12.1 µm after 10 min. This indicates that one of the dominant structural changes at the early stage of pulping is the swelling of cell walls. This likely occurs due to the transport of the cooking chemicals (in this case hydroxide ions) through lumen, resin channels and pits causing an increased pH, which implies deprotonation of carboxylic and hydroxylic groups, leading to swelling of the cell walls and a decrease of the diameter of the lumen (see Figure 5B). Further pulping to 20 min is seen to result in a slight decrease in the cell wall thickness with a clear increase of the tracheid diameter. This is inferred to be the result of gradual dissolution of the lignin and hemicelluloses in the cell walls (Wagih et al. 2021) and their transport out from the cell wall causing voids that further facilitate the transport of chemicals and dissolved constituents. During this stage of pulping, from 10 to 20 min, saturation of the inner layers of cell walls and some dissolution of lignin and hemicelluloses are expected to give a reduction of the cell wall thickness, but the swelling effect is seen to be more pronounced than the depletion of the components from the cell wall. The presence of voids in the cell walls, due to the removal of lignin and hemicelluloses, causes shrinkage of the cell walls and results in increased lumen size. These voids are also beneficial for transport of chemicals and dissolved wood components through the layers in the cell and, thus, accelerated lignin and hemicelluloses removal, which leads to faster reduction of the cell wall thickness after 30 min, as shown in Figure 5c. Thus, the dissolution of lignin and hemicelluloses is the dominant mechanism at this stage.

During soda pulping of wood, three main paths are responsible for transport of chemicals into the wood tissue that react with wood components to achieve the delignification process. Two of these paths are initially part of the wood structure, while the third is generated by the dissolution of wood components. The first path is a longitudinal path through the lumen and pits as well as resin channels. The second is radial path through pits and across the lumen diameter, which facilitates transportation between tracheids through cell walls and, to some extent, via radial rays. With increasing pulping time, dissolution of lignin and hemicelluloses occurs in the outer cross section of the sample and results in dissolution of these components from the middle lamella (between cell walls), as marked with red arrows in Figure 5C. With the removal of these components, a new transportation path is considered to have been generated via the voids in the cell walls to the middle lamella, which likely enables transport of chemicals and dissolved wood components in the radial and

tangential directions. The significant and fast (0.08 µm/min, as given by the slope of the black dash line in Figure 6) cell wall reduction observed from 20 min up to 60 min processing time is attributed to the activation of this third transport path in addition to the first two paths. The activation of these three paths speed up the reaction and, hence, allow a higher rate of dissolving wood components. This increased wall reduction rate starts at the surface of the wood chip and occurs successively inwards with increasing reaction time.

The cell wall thickness estimated from *in situ* investigation after 30 min pulping was larger than that computed from the previous *ex situ* experiments. This is most likely due to interrupting of the cooking process and taking the sample out and extensive washing that inevitably involve cooling and some desaturation, which lead to shrinkage of the cell walls that could hide some microstructure characteristics and lead to underestimation in the *ex situ* measurements of wall thickness. This highlights the importance of observing microstructure changes *in situ* during the experiment and under the processing conditions.

After 60 min pulping, the cell wall thickness reduction rate was reduced to about 0.022 µm/min (slope of the red dash line in Figure 6), which indicates change in the microstructure of the pulped wood along with continued removal of dissolved material out from the cell wall. The majority of the hemicelluloses and lignin should be dissolved from the cell walls by this time, 60 min, (Wagih et al. 2021) and the dissolution is focused in the middle lamella, which will result in decohesion between cell walls, as shown in Figure 5E. In Figure 5E, the decohesion between cell walls can be seen to be greater around the resin channel indicating that it likely occurred their first and propagated in the longitudinal direction faster than in other cell walls, due to the larger diameter of resin channel (compared to tracheids), which allows a faster transportation of delignified components and active chemicals in the longitudinal direction. It is worth noting that the cell wall thickness observed in the *in situ* tests and the *ex situ* tests are similar at this stage of processing. This is likely because the removal of the major part of the lignin and hemicelluloses occurs in the early stages of pulping (upto 30 min). After 60 min there is no significant amount of these components to be washed out, which reduce the influence of the washing of the samples in the *ex situ* experiments such that the chemicals in the cells walls are replaced by water during washing and the cell wall thickness remains unchanged.

5 Conclusions

Synchrotron phase-contrast XRT and a new laboratory reactor have been employed to perform *in situ* studies of structural changes in spruce wood during soda pulping. A reaction cell that allows recording of XRT projections while performing a continuous soda-pulping experiments was designed and manufactured such that the microstructural changes of cell walls and lumen could be followed uninterrupted and under processing conditions. The reaction cell mimics standard lab-scale experiments and industrial processes well, as it enables the required high temperature and circulation of the liquor around the samples during processing. By studying the 3D XRT images obtained at different intervals during the experiment, the evolution of morphological changes and cell wall thickness during the pulping experiment were successfully described, which cannot be done comprehensively with *ex situ* experiments. Moreover, the *in situ* imaging approach provides improved understanding on how the local morphology varies with time, as the evolution single samples can be followed, as opposed to looking at similar samples from different stages in *ex situ* studies. This is of great importance for further studies of mass transport of wood constituents as well as cooking chemicals.

Based on the obtained results, and in connection with previous studies, the cooking may be divided into different three phases.

(a) At the early stages of pulping, the first 10 min, the cell walls swell due to absorption of the alkaline cooking liquor. The active ions (OH^-) react and dissolve lignin and hemicelluloses in the secondary wall to cause the gradual formation of pores in the cell wall. These pores increase the possibility of liquor to be transported inside the cell walls, as indicated by a slight increase of the cell wall thickness in the images.
(b) After 20 min pulping, the cell wall thickness rapidly decreases due to the extensive removal of lignin and hemicelluloses from the cell walls. Moreover, lignin in the middle lamella close to the sample (wood chip) surface starts to be removed gradually, which allows faster transportation of active chemicals in the longitudinal direction and accelerates the removal of lignin and hemicelluloses. This stage extends up to 60 min.
(c) After 60 min, the cell wall thickness reduction rate is reduced, indicating a lower removal rate of lignin and hemicelluloses.

The timing and duration of the stages defined above may vary with several process conditions, including wood type, size of wood chip, cooking chemicals (soda or kraft) and temperature.

Acknowledgments: The authors acknowledge the Paul Scherrer Institute, Villigen, Switzerland for provision of synchrotron radiation beamtime at the TOMCAT beamline X02DA of the SLS. Moreover, the authors acknowledge Dr. Jonas Engqvist for helping in modifying the device to be mounted over the beamline bed. Finally, the authors acknowledge Dr. Sara Johansson for her help in performing synchrotron inspection.

Author contributions: All the authors have accepted responsibility for the entire content of this submitted manuscript and approved submission.

Research funding: The authors would like to acknowledge the ForMax pre-project initiative financed by the Swedish Government and the "FORMAX-portal - access to advanced X-ray methods for forest industry" (VR project no.: 2018-06469). V. Novak acknowledges funding from the European Union's Horizon 2020 research and innovation programme under the Marie Skłodowska-Curie Grant Agreement No. 701647.

Conflict of interest statement: The authors declare no conflicts of interest regarding this article.

References

Ahmed, S., Klassen, T.N., Keyes, S., Daly, M., Jones, D.L., Mavrogordato, M., Sinclair, I., and Roose, T. (2016). Imaging the interaction of roots and phosphate fertiliser granules using 4D X-ray tomography. Plant Soil 401: 125–134.

Baptista, C., Robert, D., and Duarte, A.P. (2006). Effect of pulping conditions on lignin structure from maritime pine kraft pulps. Chem. Eng. J. 121: 153–158.

Bale, H.A., Haboub, A., MacDowell, A.A., Nasiatka, J.R., Parkinson, D.Y., Cox, B.N., Marshall, D.B., and Ritchie, R.O. (2013). Real-time quantitative imaging of failure events in materials under load at temperatures above 1600 C. Nat. Mater. 12: 40–46.

Chakar, F.S. and Ragauskas, A.J. (2004). Review of current and future softwood kraft lignin process chemistry. Ind. Crop. Prod. 20: 131–141.

Derome, D., Griffa, M., Koebel, M., and Carmeliet, J. (2011). Hysteretic swelling of wood at cellular scale probed by phase-contrast X-ray tomography. J. Struct. Biol. 173: 180–190.

Ebner, M., Marone, F., Stampanoni, M., and Wood, V. (2013). Visualization and quantification of electrochemical and mechanical degradation in Li ion batteries. Science 342: 716–720.

Gellerstedt, G., Majtnerova, A., and Zhang, L. (2004). Towards a new concept of lignin condensation in kraft pulping. Initial results. C. R. Biol. 327: 817–826.

Gierer, J. (1980). Chemical aspects of kraft pulping. Wood Sci. Technol. 14: 241–266.

Harry, K.J., Hallinan, D.T., Parkinson, D.Y., MacDowell, A.A., and Balsara, N.P. (2014). Detection of subsurface structures underneath dendrites formed on cycled lithium metal electrodes. Nat. Mater. 13: 69–73.

Labidi, A., Robert, D., and Pla, F. (1993). Alkaline delignification of hardwoods in a flow-through reactor working at a low residence time. Part VI. Characterization of kraft poplar lignins by 13CNMR. Holzforschung 47: 213–218.

Lazarescu, C., Watanabe, K., and Avramidis, S. (2010). Density and moisture profile evolution during timber drying by CT scanning measurements. Dry. Technol. 28: 460–467.

Maire, E. and Withers, P.J. (2014). Quantitative X-ray tomography. Int. Mater. Rev. 59: 1–43.

Marone, F. and Stampanoni, M. (2012). Regridding reconstruction algorithm for real-time tomographic imaging. J. Synchrotron Radiat. 19: 1029–1037.

Muzamal, M., Bååth, J.A., Olsson, L., and Rasmuson, A.S. (2016). Contribution of structural modification to enhanced enzymatic hydrolysis and 3-D structural analysis of steam-exploded wood using X-ray tomography. Bioresources 11: 8509–8521.

Paganin, D., Mayo, S.C., Gureyev, T.E., Miller, P.R., and Wilkins, S.W. (2002). Simultaneous phase and amplitude extraction from a single defocused image of a homogeneous object. J. Microsc. 206: 33–40.

Robert, D.R., Bardet, M., Gellerstedt, G., and Lindfors, E.L. (1984). Structural changes in lignin during kraft cooking Part 3: on the structure of dissolved lignins. J. Wood Chem. Technol. 4: 239–263.

Santos, B.R., Hart, W.P., Jameel, H., and Chang, H. (2013). Wood based lignin reactions important to the biorefinery and pulp and paper industries. Bioresources 8: 1456–1477.

Scheel, M., Seemann, R., Brinkmann, M.D.M.M., Di Michiel, M., Sheppard, A., Breidenbach, B., and Herminghaus, S. (2008). Morphological clues to wet granular pile stability. Nat. Mater. 7: 189–193.

Sjöström, E. (1977). The behaviour of wood polysaccharides during alkaline pulping processes. Tappi 60: 151–154.

Tikka, P.O. and Kovasin, K.K. (1990). Displacement vs conventional batch kraft pulping – delignification patterns and pulp strength delivery. Pap. Puu 72: 773–779.

Van den Bulcke, J., Masschaele, B., Dierick, M., Van Acker, J., Stevens, M., and Van Hoorebeke, L. (2008). Three-dimensional imaging and analysis of infested coated wood with X-ray submicron CT. Int. Biodeterior. Biodegrad. 61: 278–286.

Villevieille, C., Ebner, M., Gómez-Cámer, J.L., Marone, F., Novák, P., and Wood, V. (2015). Influence of conversion material morphology on electrochemistry studied with operando X-ray tomography and diffraction. Adv. Mater. 27: 1676–1681.

Wagih, A., Maimi, P., Blanco, N., Garcia-Rodriguez, S.M., Guillamet, G., Issac, R.P., Turon, A., and Costa, J. (2019). Improving damage resistance and load capacity of thin-ply laminates using ply

clustering and small mismatch angles. Compos. Appl. Sci. Manuf. 117: 76–91.

Wagih, A., Hasani, M., Hall, S.A., and Theliander, H. (2021). Micro/nano-structural evolutions in spruce wood during soda pulping. Holzforschung 75: 754–764.

Walker, S.M., Schwyn, D.A., Mokso, R., Wicklein, M., Müller, T., Doube, M., Stampanoni, M., Krapp, H.G., and Taylor, G.K. (2014). In vivo time-resolved microtomography reveals the mechanics of the blowfly flight motor. PLoS Biol. 12: 1–12.

Walther, T. and Thoemen, H. (2009). Synchrotron X-ray microtomography and 3D image analysis of medium density fiberboard (MDF). Holzforschung 63: 581–587.

Withers, P.J. (2007). X-ray nanotomography. Mater. Today 10: 26–34.